International Journal of Fluid Mechanics Research, Vol. 31, No. 2, 2004

# Radiative Free Convective Non-Newtonian Fluid Flow past a Wedge Embedded in a Porous Medium[†]

**A. J. Chamkha**
Manufacturing Engineering Department
The Public Authority for Applied Education and Training
P. O. Box 42325, Shuweikh, 70654 Kuwait

**H. S. Takhar**
Department of Engineering
Manchester Metropolitan University
Manchester, M1 5GD, UK

**O. A. Bég**
18 Milton Grove, Whalley Range
Manchester, M16 0BP, UK

An isothermal boundary layer analysis is presented for the convection flow of a second-order non-Newtonian fluid past a two-dimensional wedge embedded in a non-Darcian porous medium in the presence of significant thermal radiation, surface transpiration and Eckert viscous heating. Nonsimilar numerical solutions are generated for the shear stresses and local heat transfer rates at the surface of the wedge using the Keller difference technique extended to a higher matrix order. It is found that the heat transfer magnitude is enhanced by an increase in the radiative flux parameter (Boltzmann – Rosseland number, $\mathrm{Bo}$), but depressed considerably with an increase in the viscoelasticity of the second-order fluid parameter, $K$. The surface shear stresses are markedly decreased with rise in the viscoelasticity parameter $K$. Conversely, surface lateral mass flux (transpiration) is seen to lower the shear stresses at the surface and to greatly boost the heat transfer there. The effects of Eckert heating are also presented graphically and discussed.

* * *

## Nomenclature

| | |
|---|---|
| $b$ | inertia coefficient of porous medium; |
| $C_F$ | dimensionless Forcheimmer second-order drag coefficient; |
| $C_p$ | specific heat at constant pressure; |
| $\mathbf{T}$ | Cauchy stress tensor; |

[†] Received 14.04.2004



ISSN 1064-2277

$\mathbf{I}$ unit tensor;
$\mathbf{A_1}$, $\mathbf{A_2}$ Rivlin – Ericksen tensors;
g acceleration due to gravity;
$\boldsymbol{V}$ velocity field vector;
$||$ modulus notation (norm for vectors, trace norm for tensors);
$k$ permeability of porous medium;
$K$ viscoelastic material parameter;
$x, y$ distances parallel to and normal to the two-dimensional wedge face;
$U$, $V$ velocities in $x$ and $y$-directions, respectively;
$U(x)$ boundary layer edge velocity (potential flow velocity outside shear layer);
$U_0$ free stream velocity;
$Q_R$ radiative energy flux;
$T$ temperature;
$T_w$ wall temperature (i. e., at the wedge surface);
$T_\infty$ free stream temperature;
Da Darcy number, $k/L^2$;
Fs Forcheimmer number, $b/L$;
$V(x)$ suction or blowing function;
$()_0$ reference condition;
Bo Boltzmann – Rosseland radiation-conduction parameter, $\kappa a_r/4\sigma T^3$;
Gr Grashof number = ratio of buoyancy to viscous hydrodynamic forces, $\mathrm{g}\beta\Delta T_0(x - x_0)/U_0^2 L$;
Re Reynolds number = ratio of inertial to viscous hydrodynamic force, $U_0 L/\nu$;
Pr Prandtl number = ratio of momentum and thermal diffusivities, $\nu/\alpha_m$;
$m$ wedge-law parameter i. e. power-law index;
$L$ reference length.

**Greek Symbols**

$\varepsilon$ porosity of the porous medium;
$\theta$ non-dimensionalized temperature = $(T - T_\infty)/(T_w - T_\infty)$;
$\kappa$ thermal conductivity of fluid-saturated porous medium;
$\alpha_1, \alpha_2$ normal stress moduli (material moduli);
$\alpha$ boundary layer parameter of unity value, for generality, $(U\delta)(\delta\nu)$;
$\beta_1$ thermal expansion coefficient;
$\beta^*$ extinction coefficient;
$\beta$ wedge parameter (pressure gradient parameter), $\dot{U}\delta^2/\nu$;
$\gamma$ suction or blowing parameter, $V\delta/\nu$;
$\mu_f$ dynamic viscosity;
$\mu'$ Brinkman effective viscosity;
$\nu$ kinematic viscosity;
$\rho_f$ density;
$\sigma$ Stefan – Boltzmann constant;
$\delta$ hydrodynamic boundary layer thickness;
$(\ )_x, (\ )_y$ denote partial differentiation with respect to $x$ and $y$ variables, respectively;
$\Delta T$ characteristic temperature difference, $\Delta T_0 |x - x_0|^{2m}/L$.

**Superscript**

$\cdot$ denotes $\partial/\partial x$

## Introduction

The evolution of new technologies in the chemical and materials processing engineering have presented new stimulating challenges to fluid dynamics research. This has occurred in parallel with advances in geophysical fluid dynamics focused on complex fluids including coastal sediments [1], slurries [2], landslide geomaterials [3], liquefied soils created following earthquakes [4] and polymer flows in petroleum reservoirs [5]. Other research into biomechanics of blood and plasma fluids has also emerged in the past several decades, as reported, for example, by Kang and Eringen [6]. Such fluids exhibit a flow behaviour which cannot be characterized by Newtonian relationships and therefore, they are referred to as non-Newtonian fluids. Most of the studies performed utilize the simpler constitutive formulations for non-Newtonian fluids, for example, Bingham plastics [7], visco-inelastic (power-law fluids) [8, 9], etc. These fluids models allow for the generation of differential equations of the boundary-layer type (parabolic) which are numerically easier to solve.

In recent years, with the advances in computing power, and simultaneous developments in more robust numerical solvers, engineering scientists have attempted more complex and realistic numerical simulations using the more advanced constitutive models for non-Newtonian fluids, as reviewed by Schowalter [10]. A large body of the literature has therefore emerged in the study of viscoelastic [11] fluids, Olroyd-B [12] fluids, and most recently second-order non-Newtonian fluids [13]. Fosdick and Rajagopal [14] have popularized the latter model and shown its applicability to a wide variety of engineering fluids. A number of papers have subsequently appeared discussing the hydrodynamics of these fluids for various geometrical configurations. Garg and Rajagopal [15] have studied the stagnation point boundary-layer flow of a second-order fluid past a flat plate. Rajagopal et al. [16] have examined the boundary-layer flow over a stretching sheet for polymer processing applications. More recently, a number of studies have emerged examining the effects of heat transfer on viscoelastic second-order fluid flows. Takhar and Bég [17] have modeled the hydromagnetic dissipative convection flow of a second-order fluid past a horizontal wedge in a porous medium. Takhar et al. [18] have tackled the problem of non-similar mixed convection flow past a vertical wedge.

Such studies have dwelled on only two of the three fundamental modes of heat transfer, namely, conduction and convection. The presence of significant thermal radiation heat transfer in various geophysical and technological systems has, however, necessitated the need to extend such studies to incorporate thermal radiation heat transfer. Examples of geophysical processes invoking the three modes of heat transfer of viscoelastic materials include volcanic flows, hydrothermal systems, and other deep-earth processes [19]. In solar engineering structures, designed by civil engineers, thermal radiation effects (due to solar energy) occur in unison with convective-conductive flows in the absorber wafers, and a variety of non-Newtonian gels and fluids are now being considered for implementation in these systems. The optimization of such systems requires advanced mathematical modeling of the processes and interaction between the various modes of heat transfer, viscoelasticity and porosity of the wafers. Some details are provided in Behling and Behling [20]. For more details regarding aerogels, the reader is referred to Heinemann and Caps [21].

Radiation effects on Newtonian convective flows have received considerable attention, both for porous and non-porous systems. Chandrasekhara and Nagaraju [22] have applied the Schuster – Schwartzchild two-flux model in their study of laminar gray fluid flow past a flat surface in a Dar-

cian porous regime. Gorla [23] has studied the transient conjugate forced convection-conduction-radiation flows in a circular pin using the diffusion approximation and solving the flow equations using the SIMPLE algorithm [24]. Bég et al. [25] have examined the effects of radiative heat transfer on non-gray gas flow in a porous medium employing the Cogley-Vincenti-Giles near-equilibrium radiative model [26]. The present study aims to consider thermal radiation effects on the more complex case of boundary-layer flow of a second-order fluid past a horizontal wedge. The Rosseland astrophysical diffusion model [27] is employed for the radiative component of heat transfer and a drag force hydrodynamic model is used for the non-Darcy effects of Brinkman-vorticity-diffusion at the wedge faces, and Forcheimmer inertial drag for higher Reynolds numbers. It should be noted that the present problem also has applications in the astrophysics of comets. Such entities comprise a dusty snowball of a mixture of frozen gases which during transport, undergo phase changes. Porosity is a very key aspect affecting the phenomena in these systems and also has an influence in meteorite and interplanetary dust systems which are highly non-Newtonian. The interested reader is referred to the excellent treatise of McDonell [28].

## 1. Physics of the Flow Problem

We consider here a second-order fluid or differential Fosdick-Rajagopal fluid. These researchers have shown that the Cauchy tensor $\mathbf{T}$ for such a fluid takes on the form:

$$\mathbf{T} = -p\mathbf{I} + \mu\mathbf{A_1} + \alpha_1\mathbf{A_2} + \alpha_2\mathbf{A_1^2}, \tag{1}$$

where

$$\mathbf{A_1} = (\operatorname{grad} \boldsymbol{V}) + (\operatorname{grad} \boldsymbol{V})^T;$$

$$\mathbf{A_2} = \frac{d\mathbf{A_1}}{dt} + \mathbf{A_1}\,(\operatorname{grad} \boldsymbol{V}) + (\operatorname{grad} \boldsymbol{V})^T\,\mathbf{A}.$$

The condition of incompressibility requires that the spherical stress be defined as above. Denotation $d/dt$ refers to the material time derivative and all other terms have been defined in the nomenclature. Dunn and Rajagopal [29] have shown that for all motions of this fluid to satisfy the Clausius – Duhelm inequality and the assumption that the specific Helmholtz free energy of the fluid is a minimum when the fluid is locally at rest, the following conditions must be satisfied.

$$\mu \geq 0, \qquad \alpha_1 \geq 0, \qquad \alpha_1 + \alpha_2 = 0. \tag{2}$$

The complete tensorial form of the equations governing flow of a second-grade fluid have been presented by Fosdick and Rajagopal [14] as:

$$\begin{gathered} \mu\Delta\boldsymbol{V} + \alpha_1\Delta\boldsymbol{V}\mathbf{I} + \alpha_1\,(\omega\Delta \times \boldsymbol{V}) + (\alpha_1 + \alpha_2) \\ \times \{\mathbf{A_1}\Delta\boldsymbol{V} + 2\operatorname{div}(\operatorname{grad}\boldsymbol{V}) + (\operatorname{grad}\boldsymbol{V})^T\} - \rho\boldsymbol{V} - \rho\,(\omega \times \boldsymbol{V}) = \operatorname{grad}P, \end{gathered} \tag{3}$$

where $\Delta$ represents the Laplacian operator.

The flow scenario under consideration in this paper concerns heat and momentum transfer through a porous material. Generally, when a fluid permeates a porous medium, the net or gross effect is described by the macroscopic Darcy law. This law, however, only simulates the resistance of a porous matrix at Reynolds numbers of less than about 10. In the present problem, we are concerned with flow characteristics near the wedge faces i. e. at the boundary interfaces of the solid geometry and the porous medium. This requires the implementation of a force term ($F_{\mathrm{Brinkman}}$) to simulate the so-called Brinkman vorticity diffusion or "Brinkman friction" at the boundaries. It can

be shown that this may be described in the parlance of boundary-layer theory by a Laplacian term of the form:

$$F_{\mathrm{Brinkman}} = \mu' \nabla^2 U, \tag{4}$$

where $\mu'$ is the Brinkman effective viscosity which is different from the viscosity of the pure percolating fluid and $U$ denotes the velocity.

The above term is essentially a viscous term and dominates the medium at lower velocities and Reynolds numbers at the interfacial boundaries. For higher velocities, neither the Darcy nor the Brinkman models are sufficient. The flow becomes inertia-dominated, and we implement the second-order drag theory propounded by Forcheimmer [30]. This takes over for Reynolds numbers beyond $10$ and introduces a quadratic retarding body force term into the boundary-layer equations. This can be expressed as:

$$F_{\mathrm{Forcheimmer}} = C_F \left| U \right| U, \tag{5}$$

where all terms have been defined in the Nomenclature section. $C_F$ is dependent on the nature of the porous medium, e. g. if it is geological, man-made, etc., as this affects the internal structure of pores. $C_F$ is, therefore, not a universal constant. More details regarding the hydrodynamic basis of the Forcheimmer model are provided by Gebhart et al. [31].

We consider also the effect of unidirectional thermal radiation on the thermal regime. This allows a much simpler approach to the thermophysics and validates the use of the Rosseland diffusion model which simplifies the mathematics of the problem considerably. Rosseland's model has proved very popular and accurate for boundary-layer convection analysis. Gorla [32] has applied this model in a Newtonian analysis of radiation effects on conjugate forced convection in a laminar wall jet along a plane surface. Gorla and Pop [33] have studied the conjugate heat transfer with radiation from a vertical circular pin to a non-Newtonian power-law fluid medium. Following Modest [34], the radiative flux term is cast as follows:

$$Q_R = -\frac{4\sigma}{3\beta^*} \frac{\partial T^4}{\partial y}\,, \tag{6}$$

where $\sigma$ is the Stefan–Boltzmann constant; $\beta^*$ is the extinction coefficient; $Q_R$ is the unidirectional radiative energy flux. The Rosseland approximation therefore allows the transformation of the governing integro-differential equation for radiative energy balance into a Fourier-type diffusion equation analogous to that describing heat conduction or electrostatic potential (Coulomb's law) which is valid for optically-thick media in which radiation only propagates a limited distance prior to experiencing scattering or absorption. It can be shown that the local intensity is caused by radiation emanating from nearby locations in the vicinity of which the emission and scattering are comparable to the location under consideration. For zones where conditions are appreciably different, the radiation has been shown to be greatly attenuated prior to arriving at the location being analyzed. The energy transfer depends only on the conditions in the area near the position under consideration. In applying the Rosseland assumption, we have assumed the following:

- refractive index of the medium is constant;
- intensity within the porous medium is nearly isotropic and uniform;
- wavelength regions exist where the optical thickness is greater than $5$.

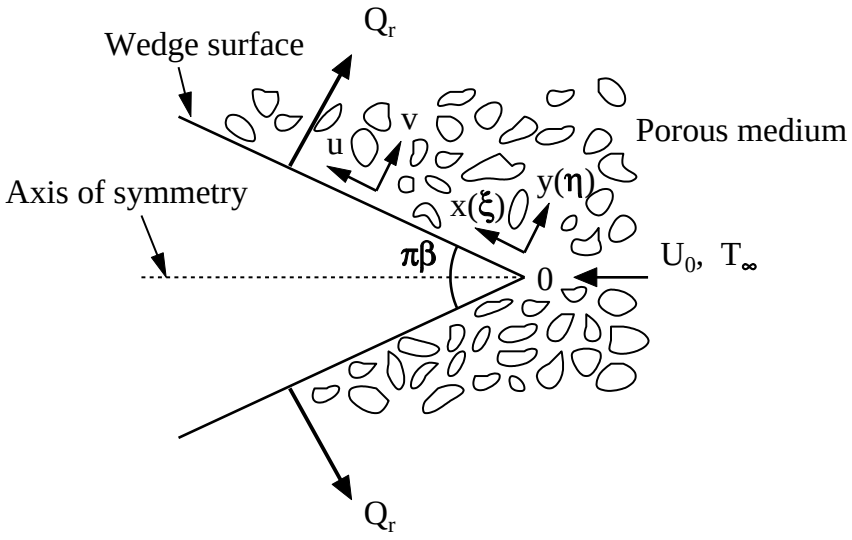


**Fig. 1.** Schematic diagram.

## 2. Mathematical Model

Our scenario concerns the two dimensional flow of an optically-thick incompressible, viscoelastic fluid past a porous horizontal wedge with an apex angle $\pi\beta$ embedded in a Darcy – Brinkman – Forcheimmer porous medium as depicted in Fig. 1. The $x$-axis is taken along the wedge faces and the $y$-axis is normal to the wedge faces. Fluid suction or injection can take place at the wedge faces into the boundary layers on either side of the wedge. Under the usual Boussinesq approximation, it may be shown that the governing convection boundary-layer equations take on the following form:

$$\begin{aligned} UU_x + VU_y = \frac{\varepsilon^2}{\rho_f}\left(-\frac{\mu_f}{k}\right)U + \rho_f \mathrm{g}\beta_1 (T - T_\infty)\sin\left(\frac{\pi\beta}{2}\right) \\ -\frac{\mu_f}{\varepsilon^2}U_{yy} - \frac{\rho_f b U^2}{k} + \frac{K}{\rho_f}\left[U_y V_{yy} + VU_{yyy} + (UU_{yy})_x + UU_x\right], \end{aligned} \tag{7}$$

$$UT_x + VT_y = \left[\frac{16\sigma T^3}{3a_r} + \kappa\right]_y T_y + \frac{\nu}{C_p}U_y^2 - \frac{UU^*}{\rho_f C_p}U_x, \tag{8}$$

where all parameters have been defined in the Nomenclature section. The appropriate hydrodynamic and thermal boundary conditions are:

$$\begin{aligned} &\text{at} \quad y = 0: \quad U(x,0) = V(x,0) = 0, \quad T(x,0) = T_w \quad \text{for} \quad x \geq 0, \\ &\text{at} \quad y \to \infty: \quad U(x,\infty) = U(x), \quad T(x,\infty) = T_\infty \quad \text{for} \quad x \geq 0. \end{aligned} \tag{9}$$

For these boundary conditions, well-posedness of the equations is at present not guaranteed since the order of the equations is one greater than for Newtonian hydrodynamics. This is due to the presence of the third-order derivative $U_{yyy}$, and the mixed third-order derivative $(U_{yy})_x$, invoked

by the viscoelastic material behavior. An augmented boundary condition is required and imposed as follows:

$$U_y(x,\infty) = 0 \quad \text{for} \quad x \geq 0. \tag{10}$$

The governing differential equations for momentum and heat transfer are nonsimilar. Introducing a pseudosimilar variable for scaling the $y$ coordinate as follows:

$$\eta = \frac{y}{\delta(x)}\,, \tag{11}$$

$$\xi = \frac{\mathrm{g}\,\beta^*\Delta T_0(x-x_0)L}{(U_0^2)^{-1}} = \frac{\mathrm{Gr}}{\mathrm{Re}^2}\,(x-x_0)\,, \tag{12}$$

where all terms have been defined in the Nomenclature section. We note that

$$\frac{\partial\xi}{\partial x} = \frac{\mathrm{Gr}}{\mathrm{Re}^2}\,. \tag{13}$$

We introduce a stream function $\psi$ as follows:

$$\psi = U(x)\delta(x)F(\xi,\eta) + \int V(x)\,dx. \tag{14}$$

From the definition of the Cauchy – Riemann equations

$$U = \frac{\partial\psi}{\partial y}\,, \qquad V = -\frac{\partial\psi}{\partial x},$$

it may be shown that:

$$U = U(x)F'(\xi,\eta), \tag{15a}$$

$$V = \frac{UF''}{\delta}, \tag{15b}$$

$$V_{yy} = \frac{UF'''}{\delta^2}, \tag{15c}$$

$$U_x = \dot{U}F' + UF'_\xi\,\xi_x - \frac{\eta\,\dot{\delta}U}{\delta}\,F'', \tag{15d}$$

where a prime indicates a partial differentiation with respect to $\eta$.

Introduction of these functions into Eqs (7) and (8) generates the coupled pseudo-similar equations for the thermal flow field which is relative to a $(\xi,\eta)$ coordinate system and take the form:

$$\begin{aligned}
&K\xi^{m-1}\left[F'''\left\{(\alpha F+\gamma)+(2\alpha-\beta)\,\xi F_\xi\right\}+(2\beta-\alpha)\left(2FF''-F''^2\right)\right.\\
&\left.+\,(2\alpha-\beta)\,\xi F''F''_\xi-(2\alpha-\beta)\,\xi F'''F'_\xi-(2\alpha-\beta)\,\xi F'F'''_\xi\right]\\
&+F'''+(\alpha F+\gamma)\,F''+\beta\left(1-F'^2\right)+\frac{\varepsilon^2}{\mathrm{DaRe}}\xi^{1-m}\,(2\alpha-\beta)\left(\frac{\mathrm{Gr}}{\mathrm{Re}^2}\right)^{m-1}F'\\
&+\varepsilon^2\xi\,(2\alpha-\beta)\sin\left(\frac{\pi\beta}{2}\,\theta\right)+\varepsilon^2\frac{\mathrm{Fs}}{\mathrm{Da}}\,\xi\,(2\alpha-\beta)\left(\frac{\mathrm{Gr}}{\mathrm{Re}^2}\right)^{-1}F'^2\\
&=(2\alpha-\beta)\,\xi\left[F'F'_\xi-F''F_\xi\right],
\end{aligned} \tag{16}$$

$$\theta''\left[1+\frac{4}{3}\,\mathrm{Bo}\,\theta^3\right]+\mathrm{Pr}\left[\alpha F+\gamma\right]\theta'+\mathrm{Pr}\,\mathrm{Ec}F''^2$$
$$-2\mathrm{Pr}\beta F'\theta+\frac{4}{\mathrm{Bo}}\,\theta^2\theta'^2=(2\alpha-\beta)\,\mathrm{Pr}\,\xi\left[F'\theta_\xi-\theta' F_\xi\right]. \tag{17}$$

The transformed conditions for this pseudo-similar two-point boundary value problem are now posed as follows:

$$\eta=0:\quad F(\xi,0)=F'(\xi,0)=0,\quad \theta(\xi,0)=1, \tag{18}$$

$$\eta=\infty:\quad F'(\xi,\infty)=1,\quad F''(\xi,\infty)=0,\quad \theta(\xi,\infty)=0. \tag{19}$$

Local skin friction and heat transfer coefficient (in terms of a local Nusselt number) may now be derived from the above derivatives. We have omitted this here. The reader is referred to the work of Bég and Takhar [35].

## 3. Numerical Simulation

The governing equations of the problem under investigation are solved numerically by the Keller-box method which is an implicit scheme with unconditional stability. The method allows for nonuniform grid discretization and converts the differential equations into algebraic ones which are then solved by the Thomas algorithm. We have used $301$ grid points in the $\xi$-direction and $196$ grid points in the $\eta$-direction. Variable step sizes in the $\eta$-direction with an initial step size of $0.001$ and a growth factor of $1.03$ and constant step size of $0.01$ in the $\xi$-direction are employed. A mesh sensitivity exercise has been performed to ensure grid independence. The solution convergence criterion required that the difference between the current and previous iterations be $10^{-5}$ or less.

## 4. Results and Discussion

The mathematical model has been solved for various data cases of practical importance and the results for the local shear stress $F''(\xi,0)$ and the local heat transfer gradient $\theta'(\xi,0)$ for various values of the spanwise coordinate $\xi$ are depicted below. We initially check the accuracy of the numerical scheme employed by comparing our results with those presented in the seminal work of Watanabe [36]. When the porosity ($\varepsilon$), Boltzmann – Rosseland radiation parameter ($\mathrm{Bo}$), viscous dissipation ($\mathrm{Ec}$), Forcheimmer drag number ($\mathrm{Fs}$), Darcy number ($\mathrm{Da}$), Grashof number ($\mathrm{Gr}$), and the viscoelastic parameter ($K$) are set to zero, our equations reduce to those solved by Watanabe [36] for forced convective thermal boundary-layer flow over a wedge, viz:

$$F'''+(\alpha F+\gamma)\,F''+\beta\left(1-F'^2\right)=(2\alpha-\beta)\,\xi\left[F'F'_\xi-F''F_\xi\right]. \tag{20}$$

For the energy equation Eq. (17) we have:

$$\theta''+\mathrm{Pr}\left[\alpha F+\gamma\right]\theta'-2\mathrm{Pr}\beta F'\theta=(2\alpha-\beta)\,\mathrm{Pr}\,\xi\left[F'\theta_\xi-\theta' F_\xi\right]. \tag{21}$$

Numerical values of $F''(0)$ (shear stress parameter) and $\theta' 3(0)$ (surface heat transfer parameter) correlate almost exactly with the earlier results of Watanabe [36]. Very good agreement is evident from [36, Table 1]) for the whole range of wedge power-law parameter $m$ ($0.0$ to $0.3333$).

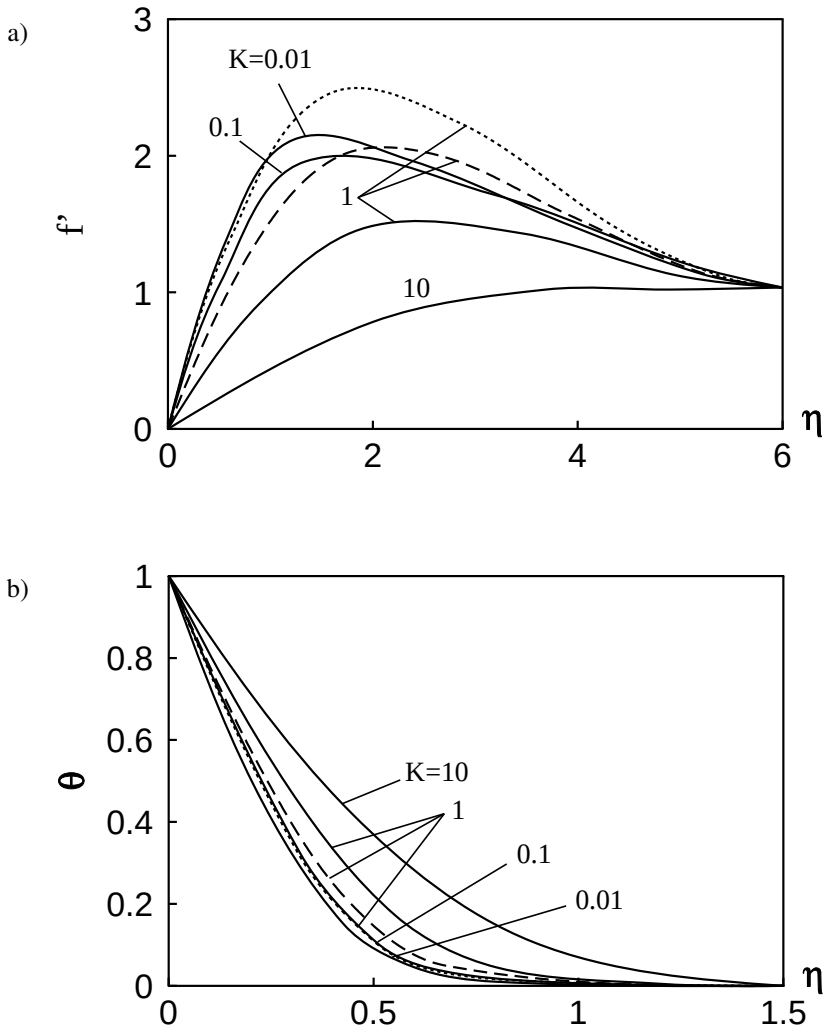


**Fig. 2.** Effects of $m$ and $\xi$ on $F''(\xi, 0)$ and $[-\theta'(\xi, 0)]$.

Since the mathematical model contains over a dozen hydrodynamic and thermo-mechanical parameters, we set some of these values to zero in order to study the effect of a single parameter on the thermo-convection flow.

Fig. 2 shows the plots of $F''(\xi, 0)$ and $[-\theta'(\xi, 0)]$ with surface coordinate ($\xi$) for various power-law wedge parameters ($m$). The value of m is related to the geometry of the flow regime. For $m = 0$, we have laminar flow past a flat surface at zero incidence e. g., horizontal geothermal stratum [$\beta/2\alpha - \beta \to 0$, $\pi\beta \to 0$]. As $m$ is elevated from $0.1429$ ($\pi\beta = 45$); $0.2$ ($\pi\beta = 60$); $0.3$ ($\pi\beta = 83$); $0.5$ ($\pi\beta = 120$), through to $0.75$ ($\pi\beta = 154.3$), for $m < 0.3333$, we have an acute included wedge angle, and for $m > 0.3333$, $\pi\beta$ is obtuse. The shear stress initially fall for $m = 0.3$, then $m = 0.2$ and $0.12429$; however, as $m$ reaches $0.5$ (and $\pi\beta$ becomes $120$) and then $m$ becomes $0.75$, we see that shear stress rises markedly. Hence, the fluid is decelerated by a rise in m up to quite high values, after which the flow begins to accelerate and the wall shear stress rises correspondingly. A more consistent pattern is observed in the case of surface heat transfer and

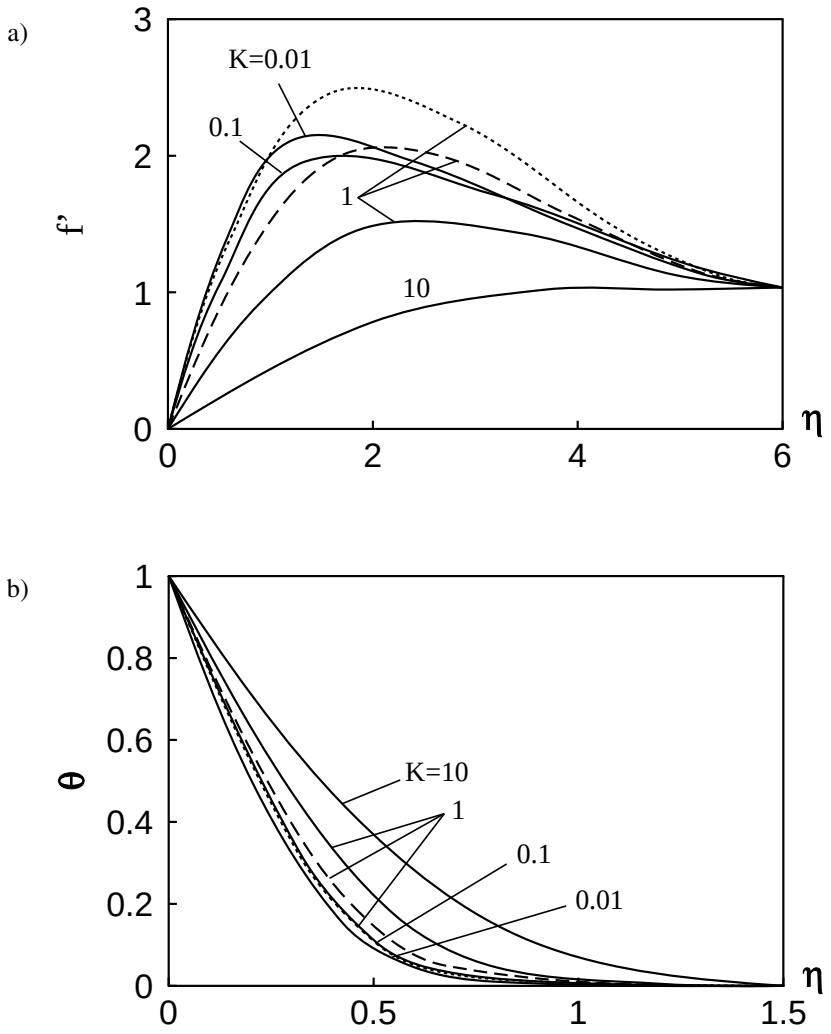


**Fig. 3.** Effects of $\gamma$ and $\xi$ on $F''(\xi,0)$ and $[-\theta'(\xi,0)]$.

$(-\theta'(\xi,0))$, which steadily increases with $m$. The parametric values employed in the computations are: $\alpha = 1$; $K = 1$; $\varepsilon = 0.6$; $\mathrm{Pr} = 10$; $\gamma = 0$; $\mathrm{Ec} = 0$; $\mathrm{Bo} = 0$; $\mathrm{Fs} = 0.055$; $\mathrm{Re} = 1$; $\mathrm{Gr} = 100$; $\mathrm{Da} = 0.01$. The case of acute wedge angles may be of use in studying molten (viscoelastic) lava flows past angular rock structures which may be intersecting.

The effects of surface transpiration $\gamma$ (material injection into the boundary layer) i. e., lateral mass influx, on $F''(\xi,0)$ and $[-\theta'(\xi,0)]$ are depicted in Fig. 3. As $\gamma$ is raised from $0$ (non-porous i. e. no transpiration) to $0.5$; $1.0$; $2.0$, a sharp increase in the wall shear stress occurs. The wall heat transfer magnitude is also seen to increase substantially.

The variations of $F''(\xi,0)$ and $[-\theta'(\xi,0)]$ versus $\xi$ for different Eckert numbers (Ec) are presented in Fig. 4. The Eckert number defines the ratio of kinetic energy of the flow relative to the enthalpy difference across the thermal boundary layer. Although it has an important role in supersonic and hypersonic aerodynamic flows (where energy dissipation is significant), it is also very

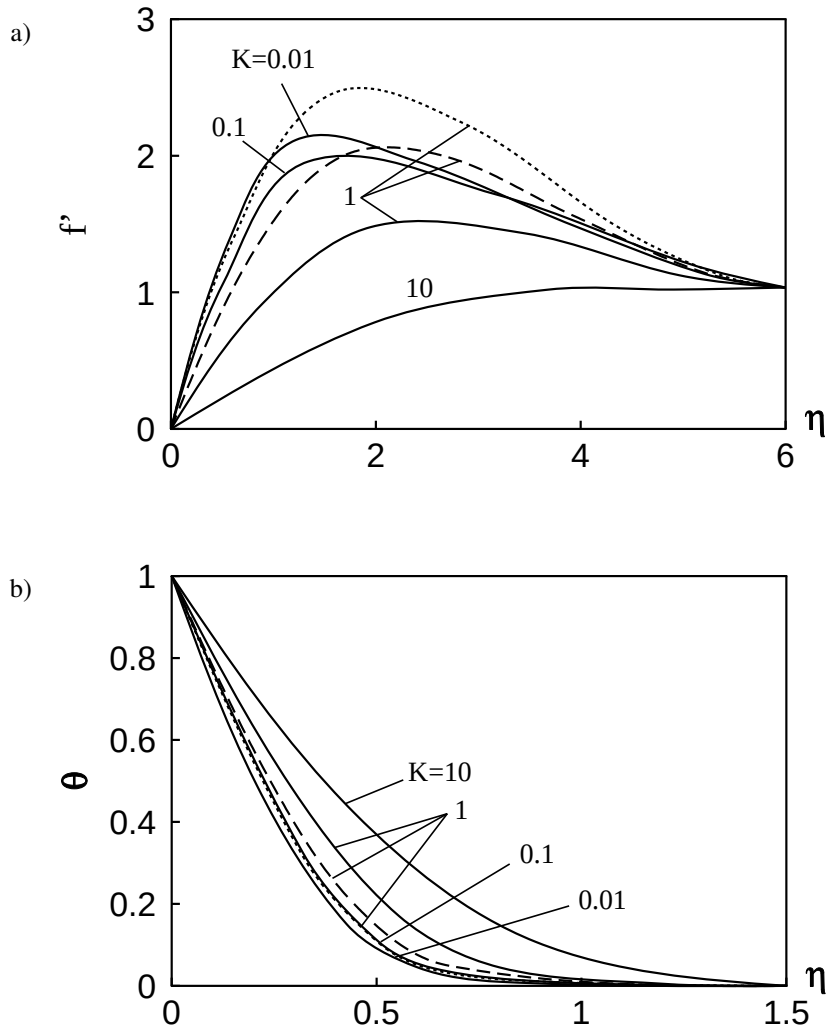


**Fig. 4.** Effects of Ec and $\xi$ on $F''(\xi,0)$ and $[-\theta'(\xi,0)]$.

important in very high temperature flows in geothermic and volcanic heat transfer systems. Positive values of Ec defines wedge face cooling and negative values of Ec defines plate heating. The viscous dissipation term in our mathematical model is given by:

$$\Pr \mathrm{Ec}\, F''^2. \tag{22}$$

This is derived from the general viscous dissipation energy effect term which is given by Gebhart et al. [31]. Viscous dissipation is also approximately the difference between the total mechanical power input by the stress system and the smaller amount of the total power input that produces thermodynamically reversible effects, for example, elevations in kinetic and potential energy. The difference is the quantity of energy dissipated as thermal energy by viscous effects. We observe that for $\mathrm{Ec} > 0$ or $\mathrm{Ec} < 0$, the surface shear stress $F''(\xi,0)$ is not noticeably affected since Ec does not appear in the momentum equation. However, $[-\theta'(\xi,0)]$ is seen to rise for negative values of Ec and depressed for positive values of Ec. Heat is conducted away from the wedge surfaces

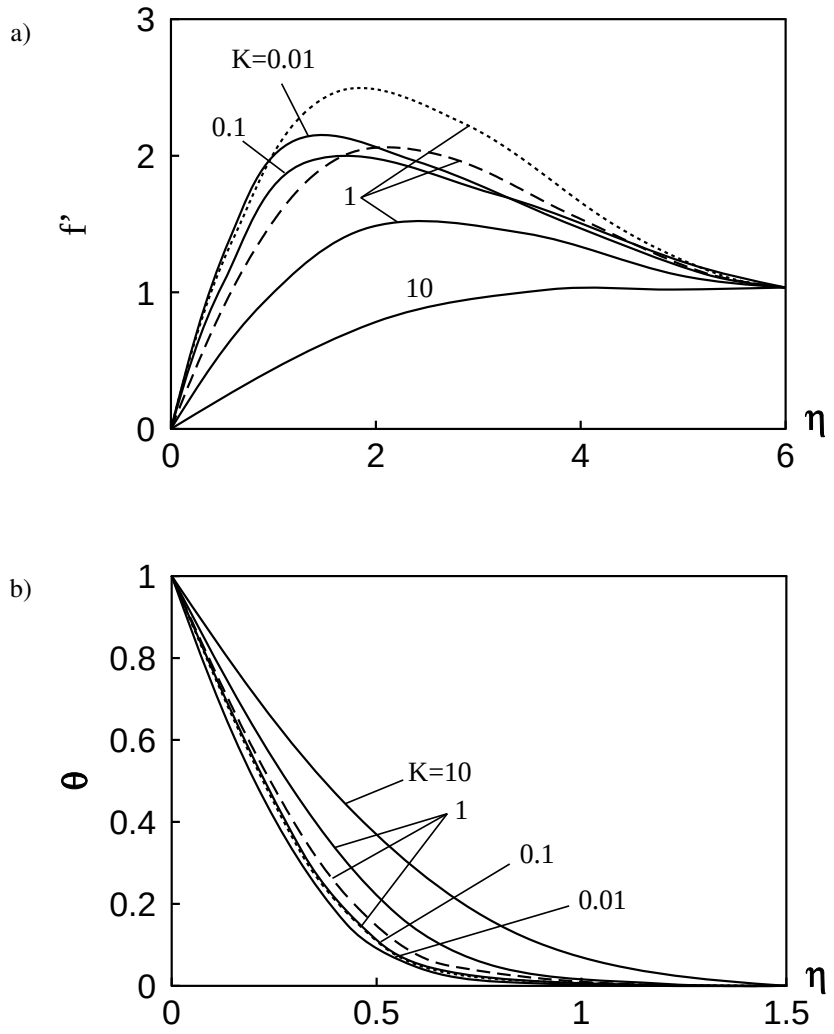


**Fig. 5.** Effects of Bo and $\xi$ on $F''(\xi,0)$ and $[-\theta'(\xi,0)]$.

for positive Ec (wedge cooling) and is being passed back to the surfaces for negative Ec (wedge heating).

Fig. 5 depicts the variations of the surface shear stress $F''(\xi,0)$ and the local heat transfer $[-\theta'(\xi,0)]$ with $\xi$ for various values of the radiation parameter (Bo). The parameter Bo encapsulates the relative role of heat transfer by the conduction mode to that by the radiative mode. For radiative heat transfer dominance in the thermal boundary layer, $\mathrm{Bo} \to 0$, so that $(4/\mathrm{Bo}) \to \infty$. Hence, higher values of $(4/\mathrm{Bo})$ imply a greater quantity of radiation heat transfer and consequent heating of the fluid. Conversely, as $\mathrm{Bo} \to \infty$, then $(4/\mathrm{Bo}) \to 0$, and the conduction mode of heat transfer dominates the flow in the energy boundary layer. Increasing Bo from $0$ to $0.2$ has no effect on the wall shear stress but depresses the heat transfer rate since conduction dominates and radiation contribution decreases. It is, therefore, apparent that as radiation rises (with $\mathrm{Bo} \to 0$), the wall heat transfer magnitude $|-\theta'(\xi,0)|$ is augmented. This is important in polymer processing of sheets and possibly basal flows of volcanic materials past rock strata, showing that the presence of radiation

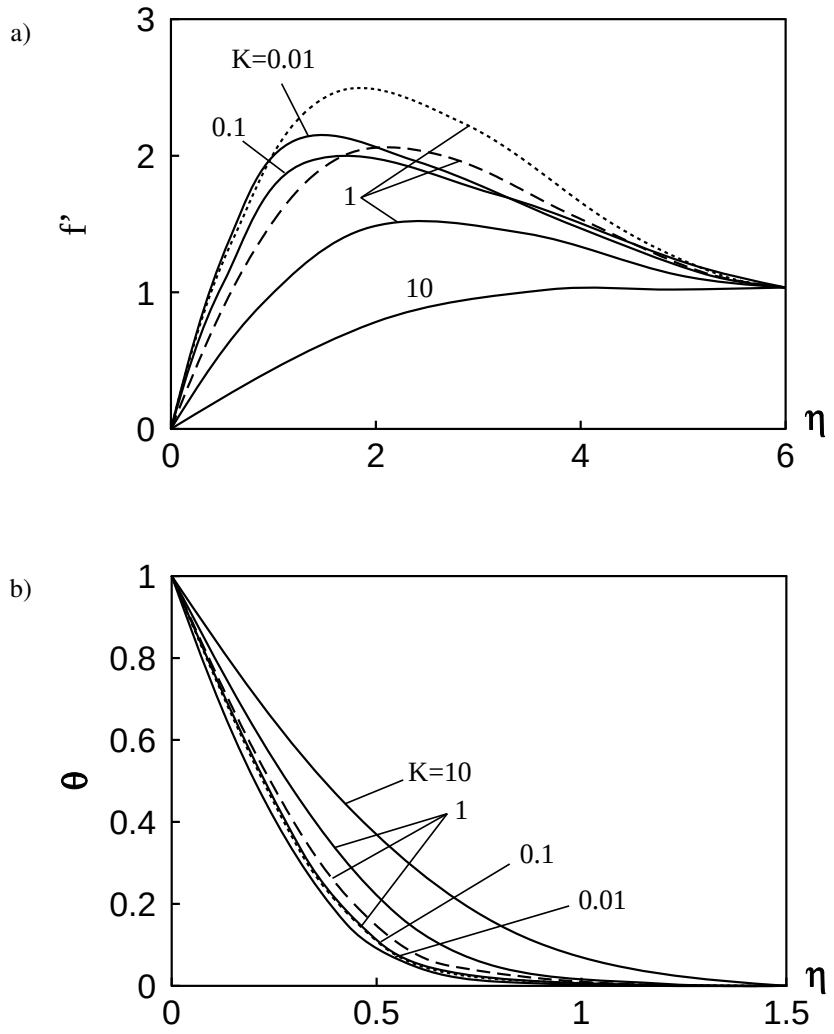


**Fig. 6.** Effects of $K$ on $f'(\xi, \eta)$ and $\theta(\xi, \eta)$.

increases the overall wall heat transfer magnitudes.

Fig. 6 illustrates the effects of the viscoelasticity parameter $K$ on the dimensionless velocity and temperature profiles plotted as we move perpendicular from the wedge surface, i. e., along the spanwise coordinate for different (streamwise) locations. Generally, the fluid velocity falls as the value of $K$ rises. As we have explained, this is due to a deceleration in the fluid due to a thickening of the velocity boundary layer due to increased viscosity effects. Conversely, the fluid temperature is seen to rise steadily with rising values of $K$ from $0.01$; $0.1$; $1.0$ to $10.0$ (polymeric fluids).

## Conclusions

In this work we have attempted to simulate nonlinear viscoelastic flows through porous industrial and geological media using a complex second-order non-Newtonian thermal boundary-layer

flow model derived from an extension to the Navier – Stokes flow equations. This was done through the study of radiative free convection flow past a wedge embedded in a porous medium in the presence of wall mass transfer and viscous dissipation. It was shown that radiation augments heat transfer in such fluids. However, the fluid viscoelasticity had a detrimental effect on the wall heat transfer. Increases in the transpiration parameter produced lower wall shear stresses and higher wall heat transfer rates. While increases in the value of the Eckert number did not produce significant changes in the wall shear stresses, it produced lower wall heat transfer rates.

## REFERENCES


1. Liu, P. L. F. and Mei, C. C., Long Waves in Shallow Water over a Layer of Bingham Plastic Fluid Mud: Physical Aspects, *Int. J. Engng Sci.*, 1993, **31**, No. 1, pp. 125–144.
2. Brenner, H., Edwards, D. A., and Wasan, T., *Interfacial Transport Processes and Rheology*, MIT, Mass., USA, 1991.
3. Philips, C. J. and Davies, T. R. H., Determining Rheological Parameters of Debris Flow Material, *Geomorphology*, 1991, **4**, pp. 101–110.
4. Locat, J. and Dmers, D., Viscosity, Yield Stress, Remoulded Strength and Liquidity Index Relationships For Sensitive Clays, *Can. Geotech. J.*, 1988, **4**, No. 25, pp. 799–806.
5. Rodriguez, S. et al., Flow of Polymer Solutions Through Porous Media, *J. Non-Newton. Fluid Mech.*, 1993, **49**, pp. 63–85.
6. Kang, C. K. and Eringen, A. C., The Effects of Microstructure on the Rheological Properties of Blood, *Bull. Math. Biol.*, 1976, **38**, pp. 135–159.
7. Hlavacek, M., The Role of Synovial Fluid Filtration by Cartilage in the Lubrication of Synovial Joints-1: Mixture Model Of Synovial Fluid, *J. Biomech.*, 1993, **26**, No. 10, pp. 1145–1150.
8. Takhar, H. S. et al., Free Convection of a Non-Newtonian Power Law Fluid from a Vertical Wavy Surface with Uniform Heat Flux, *ZAMM*, 1996, **76**, pp. 531–536.
9. Gorla, R. S. R. et al., Free Convection Power Law Fluids Near a Three Dimensional Stagnation Point, *Int. J. Heat Fluid Flow*, 1995, **16**, pp. 62–68.
10. Schowater, W. R., *Mechanics of Non-Newtonian Fluids*, Pergamon Press, Princeton Univ., USA, 1978.
11. Huilgol, R. R., *Continuum Mechanics of Viscoelastic Liquids*, John Wiley, New York, 1975.
12. Lodge, A. S., *Body Tensor Fields in Continuum Mechanics with Applications to Polymer Rheology*, Academic Press, New York, 1975.
13. Bég, O. A., *Viscoelastic Models of Volcanic and Debris Flows for Implementation in CFD Codes. Technical Report*, Manchester, Ove Arup & Partners, Consulting Engineers, March, 1999.
14. Fosdick, R. and Rajagopal, K. R., Uniqueness and Drag for Fluids of Second Grade in Steady Motion, *Int. J. Non-Linear Mech.*, 1978, **13**, pp. 131–137.
15. Garg, V. K. and Rajagopal, K. R., Stagnation Point Flow of a Non-Newtonian Fluid, *Mech. Resch Commun.*, 1990, **17**, pp. 415–421.
16. Rajagopal, K. R., Na, T. Y., and Gupta, A. S., Flow of a Viscoelastic Fluid over a Stretching Sheet, *Rheologica Acta*, 1984, **23**, pp. 213–215.
17. Bég, O. A., Takhar, H. S., Kumari, M., and Nath, G., Computational Fluid Dynamics Modelling of Buoyancy-Induced Viscoelastic Flow in a Porous Medium with Magnetic Field Effects, *Int. J. Appl. Mech. Engng*, 2001, **6**, No. 1, pp. 187–219.
18. Takhar, H. S., Kumari, M., and Nath, G., Nonsimilar Mixed Convection of a Non-Newtonian Fluid past a Wedge, *Acta Mechanica*, 1994, **113**, pp. 205–213.

19. Menke, W. G. and Abbott, D., *Geophysical Theory*, Columbia Univ. Press, New York, 1990.
20. Behling, S. and Behling, S., *Solar Power: The Evolution Of Solar Architecture*, New York, Prestel, 1996.
21. Hienemann, U. and Caps, R., Radiation-Conduction Interaction: An Investigation on Silica Aerogels, *Int. J. Heat Mass Transfer*, 1996, **39**, No. 10, pp. 2115–2130.
22. Chandrasekhar, B. C. and Nagaraju, B., Composite Heat Transfer in the Case of Steady Laminar Flow of a Gray Fluid with Small Optical Density past a Horizontal Plate Embedded in a Saturated Porous Medium, *Warme-Und-Stoff*, 1988, **23**, pp. 343–352.
23. Gorla, R. S. R., Transient Conjugate Forced Convection and Conduction in a Circular Pin under Radiative Effect, *J. Appl.Mech. Engng*, 2000, **5**, No. 3, pp. 579–581.
24. Patankar, S. V., *Numerical Heat Transfer and Fluid Flow*, Hemisphere, Washington, 1980.
25. Bég, O. A., Takhar, H. S., and Kumari, M., Computational Analysis of Coupled Radiation-Convection Non-Gray Gas Flow in a Non-Darcy Porous Medium using the Keller-Box Implicit Finite Difference Scheme, *Int. J. Energy Resch*, 1998, **22**, pp. 141–159.
26. Cogley, A. C., Vincenti, W. G., and Giles, S.E., Differential Approximation for Near-Equilibrium Flow of a Non-Gray Gas, *AIAA J.*, 1968, **6**, pp. 551–554.
27. Bég, O. A., *Radiative Transfer Models for Fire Dynamics and Solar Structures Applications. Internal Report*, Manchester, Ove Arup & Partners, Consulting Engineers, May, 1998.
28. Mcdonell, J. A. M., *Cosmic Dust*, John Wiley and Sons, Toronto, 1978.
29. Dunn, J. E. and Rajagopal, K. R., A Critical Review and Thermodynamic Analysis of Fluids of the Differential Type, *Acta Rheologica*, 1991, **22**, pp. 345–367.
30. Bear, J., *Dynamics of Fluids in Porous Media*, Dover, New York, 1988.
31. Gebhart, B., Jaluria, Y., Mahajan, R., and Sammakia, B., *Buoyancy-Induced Flows and Transport*, Hemisphere, Washington, 1988.
32. Gorla, R. S. R., *Radiative Effect on Conjugate Forced Convection in a Laminar Wall Jet along a Flat Plate. Encyclopedia Of Fluid Mechanics, Suppl. 3: Advances in Flows Dynamics*, Gulf, Texas, 1993.
33. Gorla, R. S. R. and Pop, I., Conjugate Heat Transfer with Radiation from a Vertical Cylinder Pin in a Non-Newtonian Ambient Medium, *Heat and Mass Transfer*, 1993, **28**, pp. 11–15.
34. Modest, M., *Radiation Heat Transfer*, Mcgraw Hill, New York, 1993.
35. Bég, O. A. and Takhar, H. S., Micropolar Flow in a Forcheimmer – Brinkman Porous Medium, *Acta Technica* [in press].
36. Watanabe, T., Thermal Boundary Layer Flows over a Wedge with Uniform Suction or Injection in Forced Flow, *Acta Mechanica*, 1990, **83**, pp. 119–126.

□◆◆◆□